Performance Improvement of ACO-OFDM Indoor Optical Wireless Transmissions Using Partial Pre-Equalization

Jariya Panta[*1], Non-member,
Poompat Saengudomlert[**2], and **Keattisak Sripimanwat**[***3], Members

ABSTRACT

This paper analyzes the performances and presents the benefits of partial pre-equalization for indoor optical wireless transmissions based on asymmetrically clipped optical orthogonal frequency division multiplexing (ACO-OFDM) with intensity modulation and direct detection (IM/DD). In particular, for diffuse indoor optical wireless channels, partial pre-equalization can reduce the optical transmit power over post-equalization at the same target bit error rate (BER) for point-to-point transmissions even with imperfect channel knowledge. To further improve its performance, bit loading is considered to minimize the optical transmit power of ACO-OFDM while maintaining a constant target BER. In addition, broadcast transmissions to multiple users with possibly different channel qualities are considered, where pre-equalization is not applicable. Finally, we specify an appropriate channel estimate at the transmitter for such broadcast transmissions.

Keywords: Optical wireless communications, IM/DD, OFDM, ACO-OFDM, pre-equalization, post-equalization, partial pre-equalization.

1. INTRODUCTION

Recently, optical wireless communications (OWC) has emerged as an alternative to using radio frequencies (RF) for wireless communications. OWC has conventionally used infrared (IR) transmitters. This is because infrared systems present certain advantages over RF systems for short-range indoor communications, including no electromagnetic interference concerns, ease of signal confinement for security purposes, and license-free operations [1]. However, the use of white light emitting diodes (LEDs) is increasingly becoming an attractive alternative to IR since white LEDs can be used to illuminate and communicate at the same time. OWC systems using white LEDs are referred to as visible light communications (VLC) [2–4].

There are a few notable advantages of optical frequencies. They provide practically unlimited and license-free bandwidth to access, up to several hundred THz. IR and visible light provide higher security than RF since both types of signals do not penetrate through walls, and do not get interfered from other rooms or buildings. Both can be used in areas where RF communications is restricted, such as hospitals and airplanes. Nevertheless, OWC still possesses some drawbacks. One restriction is that the available optical transmit power is limited by eye-safety standards [1–5].

In indoor OWC, transmitted data signals can be degraded by multipath propagation, causing OWC channels to be frequency selective at high data rates, and leading to inter-symbol interference (ISI) [5]. To overcome this problem, orthogonal frequency division multiplexing (OFDM), which is now widely used as multi-carrier modulation in both wireline and wireless communications, is employed since OFDM provides a good protection against ISI. OFDM is not only used in RF wireless technology, but is also increasingly used in OWC wireless technology [6].

For data transmissions with IM/DD, OFDM signals must be real and non-negative, namely unipolar, whereas transmitted signals of traditional OFDM are bipolar [6]. There are a few known techniques to make OFDM signals unipolar, including DC biased optical OFDM (DCO-OFDM), asymmetrically clipped optical OFDM (ACO-OFDM), and flip-OFDM. These techniques apply the Hermitian symmetry together with the use of inverse fast Fourier transform (IFFT) to generate real OFDM signals from quadrature amplitude modulation (QAM) symbols transmitted on OFDM subcarriers [7, 8].

In [7–9], the authors compare the performances of DCO-, ACO- and flip-OFDM. ACO-OFDM is more power efficient than DCO-OFDM except for very large constellations such as 1024-QAM and 4096-QAM, which are not commonly used in practical OWC systems. This is because, for the same transmission requirement, DCO-OFDM adds a DC bias

Manuscript received on September 11, 2015 ; revised on December 21, 2015.
* Faculty of Industrial Technology , Ubon Ratchathani Rajabhat University (UBRU), Thailand, E-mail : jariya.panta@gmail.com[1]
** Center of Research in Optoelectronics, Communications and Control Systems (BU-CROCCS), Bangkok University, Thailand, E-mail : poompat.s@bu.ac.th[2]
*** LED-SmartCoN.Org, Thailand, E-mail : keattisak.sripimanwat@gmail.com[3]

that increases the optical transmit power, while ACO-OFDM uses negative clipping to avoid using a DC bias. As an alternative unipolar technique, flip-OFDM separates positive parts and negative parts of OFDM signals to be transmitted in the first and second subframes of OFDM symbols, respectively. Flip-OFDM provides the same power efficiency and spectral efficiency as ACO-OFDM [7].

Consider a receiver in the presence of a dispersive OWC channel and additive white Gaussian noise (AWGN). An OFDM receiver needs a means for compensating for ISI, which can be achieved using a one-tap equalizer. Even though traditional downlink OFDM transmissions employ post-equalization by dividing the received signals by the subcarrier gains at the receiver, post-equalization can suffer from noise enhancement [6, 10–12]. In [13], pre-equalization is shown to help reduce the required optical transmit power for a given BER target in comparison to post-equalization for diffuse indoor OWC channels. In addition, while pre-equalization may affect the peak-to-average power ratio (PAPR) of OFDM signals, simulation results in [13] indicate that pre-equalization outperforms post-equalization in terms of the BER when transmitted signals are subject to signal clipping beyond a limited signal dynamic range at the transmitter.

However, pre-equalization is only applicable if the channel is known to the transmitter. In addition, it is not applicable for broadcasting to multiple receivers [10, 11, 13, 14]. Partial pre-equalization is therefore proposed in this paper to overcome these limitations of pre-equalization. The preliminary version of the paper was presented in [15].

In particular, this paper presents the following contributions on the ACO-OFDM technique using partial pre-equalization.

- For performance analysis, we derive the BER expression for partial pre-equalization that is shown to be accurate through a close match with simulation results for dispersive OWC channels.
- BER performance analysis is carried out taking into account two separate cases, with bit loading and without bit loading, where square QAM constallations are used.
- We investigate the choice of channel estimate for the delay spread ranging from 2 to 20 ns, which is the typical range as pointed out in [1, 13, 14].

The rest of the paper is organized as follows. Section 2 presents the system model of ACO-OFDM transmissions with IM/DD, including the OWC channel models and the proposed partial pre-equalization technique. Section 3 analyzes the BER performance of ACO-OFDM using post-equalization, pre-equalization and partial pre-equalization without bit loading. Section 4 describes the bit loading algorithm used to improve the power efficiency. Section 5 presents the BER analysis for ACO-OFDM with bit loading. Section 6 provides numerical results, both from analysis and from simulation experiments, which demonstrate the attractiveness of partial pre-equalization for the single-user case as well as for broadcast transmissions to multiple users. Finally, Section 7 summarizes our contribution.

2. SYSTEM MODEL

In an ACO-OFDM system with N subcarriers, for each OFDM symbol, there are $N/4$ QAM symbols transmitted on the first half of odd-numbered subcarriers. Assume that square QAM constellations are used, and are denoted by $M \times M$ QAM, where $M \in \{2, 4, 8, 16\}$. Let S_k denote the QAM symbol on subcarrier k, where $k \in \{1, 3, ..., N/2-1\}$. The transmitted QAM symbols are [16]

$$0, S_1, 0, S_3, ..., S_{N/2-1}, 0, S^*_{N/2-1}, 0, S^*_{N/2-3}, 0, ..., S^*_1$$

The even-numbered subcarriers are not used. Note that, by using only $N/4$ independent QAM symbols on the first half of odd-numbered subcarriers, a real OFDM signal is obtained through the Hermitian symmetry property [7, 13] as follows.

$$\begin{aligned} &S_0 = S_{N/2} = 0 \\ &S_{N-k} = S^*_k,\ k \in \{1, \ldots, N/2-1\} \end{aligned}$$

The symbol S^*_k denotes the complex conjugate of S_k. Let s_n's be the time-domain samples, which are transmitted during one OFDM symbol such that $s_0, s_1, ..., s_{N-1}$ are obtained from $S_0, S_1, ..., S_{N-1}$ through the IFFT operation. As in [6, 17], the definitions of the IFFT and FFT are

$$s_n = \frac{1}{\sqrt{N}} \sum_{k=0}^{N-1} S_k e^{i2\pi kn/N},\ n \in \{0, \ldots, N-1\} \quad (1)$$

$$S_k = \frac{1}{\sqrt{N}} \sum_{n=0}^{N-1} s_n e^{-i2\pi kn/N},\ k \in \{0, \ldots, N-1\} \quad (2)$$

Using only odd-numbered subcarriers together with the Hermitian symmetry yields the following negative symmetry: $s_{N/2+n} = -s_n,\ n \in \{0, 1, \ldots, N/2-1\}$ [18]. To prevent ISI and inter-carrier interference (ICI), the signals in time domain contain the cyclic prefix (CP) at the header of each OFDM symbol, where the length of CP must be at least the length of channel impulse response (CIR). The transmitted signals with the CP can be written as

$$\underbrace{s_{N-N_{\mathrm{CP}}}, \ldots, s_{N-1}}_{\mathrm{CP}}, s_0, \ldots, s_{N-1}$$

where N_{CP} is the length of CP. Let s^+_n denote the positive parts of s_n. To make s_n's non-negative, the negative clipping function is employed, which is denoted by $s^+_n = \max(s_n, 0)$. From $s_{N/2+n} = -s_n$, the

negative parts can be clipped without losing information. The transmitted signals with the CP added and negative values clipped can be presented as

$$\underbrace{s^+_{N-N_{\rm CP}},\ldots,s^+_{N-1}}_{\rm CP},s^+_0,\ldots,s^+_{N-1}$$

Let $p(t)$ be a unit-norm rectangular pulse used to transmit the signal values as given below.

$$p(t)=\begin{cases}1/\sqrt{T}, & t\in[0,T)\\ 0, & \text{otherwise}\end{cases}$$

The transmitted optical data signal with the pulse period T for one OFDM symbol can be expressed as

$$s_{\rm opt}(t)=\alpha_{\rm W/A}\sum_{n=-N_{\rm CP}}^{N-1}s^+_{n \bmod N}p(t-nT) \qquad (3)$$

where $\alpha_{\rm W/A}$ is the conversion factor from electrical to optical domains (in W/A) of an LED-based transmitter, and $T=T_{\rm s}/(N+N_{\rm CP})$, where $T_{\rm s}$ is the OFDM symbol period.

Note that, based on the assumed rectangular pulse shape, the corresponding electrical signal (i.e., $s_{\rm opt}(t)$ in (3) without the factor $\alpha_{\rm W/A}$) has signal amplitudes equal to $s^+_{n \bmod N}/\sqrt{T}$ for $n\in\{-N_{\rm CP},\ldots,N-1\}$.

In a typical indoor environment, optical wireless transmissions can be operated in two modes: directed or line-of-sight (LOS) and non-directed or diffused. This paper assumes that the propagation of optical power depends on the multipath dispersion where light is reflected from the ceiling or some other diffusely reflecting surfaces. The CIRs according to the ceiling-bounced model and the exponential-decay model adopted in [1, 7, 14, 17] are widely used to model indoor OWC channels when the transmitted light is captured through single and multiple optical reflections. The impulse responses of ceiling-bounced and exponential models are defined as

ceiling-bounced model,

$$h(t)=H(0)\frac{6a^6}{(t+a)^7}u(t) \qquad (4)$$

exponential model,

$$h(t)=H(0)\frac{1}{D}e^{-t/D}u(t) \qquad (5)$$

In the above CIR expressions, $H(0)$ is the DC gain, D is the delay spread, $u(t)$ is the unit-step function, and $a=12\sqrt{\frac{11}{13}}D$.

At the receiver, in the presence of AWGN denoted as $n(t)$ with power spectral density $N_0/2$, the received signal in the electrical domain is

$$r(t)=\alpha_{\rm A/W}s_{\rm opt}(t)*h(t)+n(t) \qquad (6)$$

In (6), $\alpha_{\rm A/W}$ is the receiver's sensitivity (in A/W). For convenience, the discrete-time CIR is considered as $h_n,\ n\in\{0,\ldots,L-1\}$ where L is the length of CIR. It is obtained from the samples of the matched filter output, which is $h_n=[(h(t)*p(t))*p(-t)]_{t=nT}$.

The received signals after matched filtering and sampling are

$$\underbrace{r^+_{N-N_{\rm CP}},\ldots,r^+_{N-1}}_{\rm CP},r^+_0,\ldots,r^+_{N-1}$$

Let $r^+_0,...,r^+_{N-1}$ be the received signals after the CP is ignored. In the frequency domain, the output signals from the FFT of $r^+_0,...,r^+_{N-1}$ can be written as

$$R_k=0.5\alpha_{\rm W/A}\alpha_{\rm A/W}\sqrt{N}H_kS_k+N_k,\quad k\in\{1,3,\ldots,N/2-1\} \qquad (7)$$

From the above equation, the signal amplitude is reduced by half due to power loss from negative clipping, which is shown as the factor of 0.5, $\sqrt{N}$ is the factor from the definition of the FFT, H_k's are the subcarrier gains, and N_k's are the electrical noises which are independent and identically distributed (IID) circularly symmetric complex Gaussian with mean 0 and variance $N_0/2$. To recover the information bits, the received QAM symbols are demapped using Gray-coded signal constellations [19].

3. BER PERFORMANCE ANALYSIS

To calculate the signal-to-noise ratio (SNR) with the BER requirement of 10^{-5}, the minimum received electrical SNR can be calculated using the union bound estimate on the BER as follows [19]

$${\rm BER}\approx\frac{2(M-1)}{M\log_2 M}Q\left(\sqrt{\frac{6\log_2 M}{(M^2-1)}\frac{E'_{\rm b}}{N'_0}}\right) \qquad (8)$$

where $M=2^{b/2}$, and b is the number of bits per QAM symbol, $E'_{\rm b}$ and N'_0 are the energy per bit and the noise variance parameter at the receiver respectively. The function $Q(\cdot)$ is defined as $Q(x)=1/\sqrt{(2\pi)}\int_x^\infty e^{-z^2/2}dz$. Assume for now that $M\times M$ QAM constellations are used on all N subcarriers; the case with different constellations on different subcarriers is considered in a later section.

3.1 BER Analysis for Post-Equalization

For post-equalization, according to [6, 12, 13], R_k is equalized by $0.5\alpha_{\rm W/A}\alpha_{\rm A/W}\sqrt{N}H_k$ at the receiver. Hence, the received and equalized QAM symbols can be written as

$$R'_k=S_k+\frac{N_k}{(0.5\alpha_{\rm W/A}\alpha_{\rm A/W}\sqrt{N}H_k)} \qquad (9)$$

where $k\in\{1,3,\ldots,N/2-1\}$. In (9), $E'_{\rm b}=d^2(M^2-1)/12\log_2 M$, where d is the minimum distance between signal points and $N'_0=N'_{0,k}=$

$4/\alpha_{\mathrm{W/A}}^2\alpha_{\mathrm{A/W}}^2 N|H_k|^2 \times N_0/2$, where $N'_{0,k}$ denotes the noise variance on subcarrier k. Using the union bound estimate in (8), the BER for using post-equalization is estimated as

$$\mathrm{BER}_{\mathrm{post}} \approx \frac{1}{N/4}\sum_{k=1,3,\ldots}^{N/2-1}\frac{2(M-1)}{M\log_2 M}\times Q\left(\sqrt{\frac{N}{N_0}}\frac{\alpha_{\mathrm{W/A}}\alpha_{\mathrm{A/W}}|H_k|}{2}d\right) \quad (10)$$

3.2 BER Analysis for Pre-Equalization

For pre-equalization [12, 13], R_k is equalized by $\alpha_{\mathrm{W/A}}\alpha_{\mathrm{A/W}}$ at the receiver while S_k is equalized by $0.5\sqrt{N}H_k$ at the transmitter. Hence, the received and equalized QAM symbols can be written as

$$R'_k = S_k + \frac{N_k}{(\alpha_{\mathrm{W/A}}\alpha_{\mathrm{A/W}})} \quad (11)$$

where $k \in \{1, 3, \ldots, N/2-1\}$. In (11), $E'_{\mathrm{b}} = d^2(M^2-1)/12\log_2 M$ and $N'_0 = 1/\alpha_{\mathrm{W/A}}^2\alpha_{\mathrm{A/W}}^2 \times N_0/2$. Using the union bound estimate in (8), the BER for using pre-equalization is estimated as

$$\mathrm{BER}_{\mathrm{pre}} \approx \frac{2(M-1)}{M\log_2 M}Q\left(\sqrt{\frac{1}{N_0}}\alpha_{\mathrm{W/A}}\alpha_{\mathrm{A/W}}d\right) \quad (12)$$

3.3 BER Analysis for Partial Pre-Equalization

This paper proposes the use of partial pre-equalization to overcome the limitation of pre-equalization. In particular, partial pre-equalization can be used in broadcast systems, and does not require the exact channel knowledge at the transmitter. For partial pre-equalization, R_k is equalized by $\alpha_{\mathrm{W/A}}\alpha_{\mathrm{A/W}}H_k/\widehat{H}_k$ at the receiver while S_k is equalized by $0.5\sqrt{N}\widehat{H}_k$ at the transmitter, where $\widehat{H}_k$ is the subcarrier gain estimate. Based on the above partial pre-equalization procedure, the received and equalized QAM symbols can be written as

$$R'_k = S_k + \frac{N_k}{(\alpha_{\mathrm{W/A}}\alpha_{\mathrm{A/W}}H_k/\widehat{H}_k)} \quad (13)$$

where $k \in \{1, 3, \ldots, N/2-1\}$. In this paper, we assume that some channel estimation techniques are being used, and that the estimate at the transmitter (i.e., $\widehat{H}_k$) may be inaccurate. In practice, it can be approximated from some typical value. However, we assume that the receiver can estimate the channel perfectly, i.e., H_k is known to the receiver. The details of channel estimation are beyond the scope of this paper. Note that, in a scenario where data signals are transmitted to multiple users, even with perfect knowledge of subcarrier gains with respect to all the receivers, the transmitter needs to select only one gain value for each subcarrier to perform pre-equalization. One problem considered in this paper is how to select subcarrier gains so that mutiple receivers can be supported.

In (13), $E'_{\mathrm{b}} = d^2(M^2-1)/12\log_2 M$ and $N'_0 = N'_{0,k} = 1/(\alpha_{\mathrm{W/A}}^2\alpha_{\mathrm{A/W}}^2|H_k|^2/|\widehat{H}_k|^2) \times N_0/2$, where $N'_{0,k}$ denotes the noise variance on subcarrier k. Using the union bound estimate in (8), the BER for using partial pre-equalization is estimated as

$$\mathrm{BER}_{\mathrm{partial}} \approx \frac{1}{N/4}\sum_{k=1,3,\ldots}^{N/2-1}\frac{2(M-1)}{M\log_2 M}\times Q\left(\sqrt{\frac{1}{N_0}}\frac{\alpha_{\mathrm{W/A}}\alpha_{\mathrm{A/W}}|H_{\mathrm{k}}|}{|\widehat{H}_k|}d\right) \quad (14)$$

3.4 Computation of BER in Terms of the Optical Transmit Power

As in [5, 19], the optical power can be computed as $\alpha_{\mathrm{W/A}}\sigma_s/\sqrt{2\pi T}$, where σ_s is the standard deviation of s_n and can be computed as in [14] to be equal to

$$\sigma_s = \sqrt{\frac{2}{N}\sum_{k=1,3,\ldots}^{N/2-1}E_{\mathrm{s},k}} \quad (15)$$

where $E_{\mathrm{s},k}$ denotes the symbol energy on subcarrier k, where $k \in \{1, 3, \ldots, N/2-1\}$. Thus, the mean optical transmit power is

$$P_{\mathrm{opt}} = \alpha_{\mathrm{W/A}}\sqrt{\frac{1}{\pi NT}\sum_{k=1,3,\ldots}^{N/2-1}E_{\mathrm{s},k}} \quad (16)$$

From (9), $E_{\mathrm{s},k}^{\mathrm{post}} = d^2(M^2-1)/6$. Hence, the mean optical transmit power is

$$P_{\mathrm{opt}}^{\mathrm{post}} = \alpha_{\mathrm{W/A}}\sqrt{\frac{1}{\pi NT}\frac{N}{4}\frac{d^2(M^2-1)}{6}} \quad (17)$$

From (11), $E_{\mathrm{s},k}^{\mathrm{pre}} = d^2(M^2-1)/6 \times 4/(N|H_k|^2)$. Hence, the mean optical transmit power is

$$P_{\mathrm{opt}}^{\mathrm{pre}} = \alpha_{\mathrm{W/A}}\sqrt{\frac{1}{\pi NT}}\times\sqrt{\sum_{k=1,3,\ldots}^{N/2-1}\frac{d^2(M^2-1)}{6}\frac{4}{N|H_k|^2}} \quad (18)$$

From (13), $E_{\mathrm{s},k}^{\mathrm{partial}} = d^2(M^2-1)/6 \times 4/(N|\widehat{H}_k|^2)$. Hence, the mean optical transmit power is

$$P_{\mathrm{opt}}^{\mathrm{partial}} = \alpha_{\mathrm{W/A}}\sqrt{\frac{1}{\pi NT}}\times\sqrt{\sum_{k=1,3,\ldots}^{N/2-1}\frac{d^2(M^2-1)}{6}\frac{4}{N|\widehat{H}_k|^2}} \quad (19)$$

Note that the BER expressions in (10), (12), (14) are in terms of the minimum distance, d. To calculate

the BER in terms of the optical transmit power, d can be written in terms of the optical transmit power using (17), (18), (19) with $T = (N/4) \times 2\log_2 M/((N + N_{\mathrm{CP}})R)$. Accordingly, each BER expression can be written as

- BER of ACO-OFDM with Post-equalization

$$\mathrm{BER}_{\mathrm{post}} \approx \frac{8(M-1)}{NM\log_2 M} \times \sum_{k=1,3,\ldots}^{N/2-1} Q\left(\sqrt{\frac{3\pi N \log_2 M}{(1+N_{\mathrm{CP}}/N)R(M^2-1)N_0}} \times \alpha_{\mathrm{A/W}}|H_k|P_{\mathrm{opt}}\right) \quad (20)$$

- BER of ACO-OFDM with Pre-equalization

$$\mathrm{BER}_{\mathrm{pre}} \approx \frac{2(M-1)}{M\log_2 M} \times Q\left(\sqrt{\frac{3\pi \log_2 M}{4N_0(M^2-1)(1+N_{\mathrm{CP}}/N)R}} \times \sqrt{\frac{1}{\sum_{k=1,3,\ldots}^{N/2-1} \frac{1}{|H_k|^2}}}\alpha_{\mathrm{A/W}} N P_{\mathrm{opt}}\right) \quad (21)$$

- BER of ACO-OFDM with Partial pre-equalization

$$\mathrm{BER}_{\mathrm{partial}} \approx \frac{8(M-1)}{NM\log_2 M} \times \sum_{k=1,3,\ldots}^{N/2-1} Q\left(\sqrt{\frac{3\pi \log_2 M}{4N_0(M^2-1)(1+N_{\mathrm{CP}}/N)R|\widehat{H}_k|^2}} \times \sqrt{\frac{1}{\sum_{l=1,3,\ldots}^{N/2-1} \frac{1}{|\widehat{H}_l|^2}}} N\alpha_{\mathrm{A/W}}|H_k|P_{\mathrm{opt}}\right) \quad (22)$$

4. BIT LOADING TECHNIQUE FOR PERFORMANCE IMPROVEMENT OF ACO-OFDM

A margin adaptive (MA) approach is used to minimize the optical transmit power subject to the constraint on a fixed number of bits transmitted per OFDM symbol and a fixed target BER [18, 20]. Based on the water filling algorithm, bits are first loaded to the subcarriers with the minimum levels of noise normalized by the subcarrier gains. Assume that 2 bits are loaded in each step so that square QAM constellations are used on all active subcarriers. For $k \in \{1, 3, ..., N/2-1\}$, let $E'_{\mathrm{b},k}$ be the energy per bit on subcarrier k at the receiver. From the union bound estimate on the BER [19],

$$\mathrm{BER}_k \approx \frac{2(M_k-1)}{M_k \log_2 M_k} Q\left(\sqrt{\frac{6\log_2 M_k}{(M_k^2-1)}\frac{E'_{\mathrm{b},k}}{N'_{0,k}}}\right) \quad (23)$$

where $M_k = 2^{b_k/2}$, and b_k is the number of bits loaded on subcarrier k.

Since bit loading is done by the transmitter, we assume that the procedure is based on the subcarrier gain estimate $|\widehat{H}_k|$ for $k \in \{1, 3, ..., N/2-1\}$, which is available at the transmitter, instead of the actual subcarrier gain $|H_k|$. The description of the bit loading procedure is based on the normalized noise variances, which are computed by dividing the noise power, by the subcarrier gains.

The bit loading procedure based on water filling can be described as follows. First, calculate the initial water level for each k, which is set equal to $N'_{0,k}$, as

$$N'_{0,k} = \frac{2N_0}{\alpha^2_{\mathrm{W/A}}\alpha^2_{\mathrm{A/W}} N|\widehat{H}_k|^2} \quad (24)$$

Second, set the initial number of bits loaded to $b_k = 0$ for all k. Third, set the water level $W_k = N'_{0,k}$ for all k. Next, search for the lowest water level, and load 2 bits to the subcarrier with the lowest level. For this subcarrier k, update the value of b_k to $b_k + 2$. Then, calculate the transmit energy per bit $E'_{\mathrm{b},k}$ using (23) with the BER requirement of 10^{-5}, and update the new water level to $W_k = N'_{0,k} + (2\log_2 M_k)E'_{\mathrm{b},k}$, where $(2\log_2 M_k)E'_{\mathrm{b},k}$ is the signal power. Finally, repeat the process until the total number of allocated bits is equal to the target number of bits per OFDM symbol.

5. BER PERFORMANCE ANALYSIS WITH BIT LOADING

The same approach as in Section 3 can be used to calculate the average BER of ACO-OFDM with bit loading, with b_k's defined as the weight factors for averaging over subcarriers, yielding the BER expression

$$\mathrm{BER}_{\mathrm{ACO}} \approx \sum_{k=1,3,\ldots}^{N/2-1} \frac{b_{\mathrm{k}}}{b_{\mathrm{OFDM}}} \mathrm{BER}_k \quad (25)$$

where b_{OFDM} is the target number of bits transmitted per OFDM symbol.

5.1 BER Analysis for Post-Equalization with Bit Loading

In (9), $E'_{\mathrm{b,k}} = d^2(M_k^2-1)/12\log_2 M_k$ and $N'_{0,k} = 4/\alpha^2_{\mathrm{W/A}}\alpha^2_{\mathrm{A/W}} N|H_k|^2 \times N_0/2$. Following the union bound estimate in (25), the BER for using post-equalization is estimated as

$$\mathrm{BER}_{\mathrm{post}} \approx \frac{4}{b_{\mathrm{OFDM}}} \sum_{k=1,3,\ldots}^{N/2-1} \frac{(M_k-1)}{M_k} \times Q\left(\sqrt{\frac{N}{N_0}}\frac{\alpha_{\mathrm{W/A}}\alpha_{\mathrm{A/W}}|H_k|}{2} d\right) \quad (26)$$

Next, the optical transmit power can be computed as (16), where $E_{\mathrm{s},k}^{\mathrm{post}} = d^2(M_k^2-1)/6$ using (9). Hence, the mean optical transmit power is

$$P_{\mathrm{opt}}^{\mathrm{post}} = \alpha_{\mathrm{W/A}}\sqrt{\frac{1}{\pi NT}\sum_{k=1,3,\ldots}^{N/2-1}\frac{d^2(M_k^2-1)}{6}} \quad (27)$$

The finalized BER expression in terms of the optical transmit power and the transmission bit rate can be obtained by substituting d in (27) to (26), and substituting $T = b_{\mathrm{OFDM}}/(N+N_{\mathrm{CP}})R$, where R is the data rate. Thus, the BER expression can be presented as follows.

$$\mathrm{BER}_{\mathrm{post}} \approx \frac{4}{b_{\mathrm{OFDM}}}\sum_{k=1,3,\ldots}^{N/2-1}\frac{(M_k-1)}{M_k}\times Q\left(\sqrt{\frac{3\pi N b_{\mathrm{OFDM}}}{2N_0(1+N_{\mathrm{CP}}/N)R\sum_{l=1,3,\ldots}^{N/2-1}(M_l^2-1)}}\times \alpha_{\mathrm{A/W}}|H_k|P_{\mathrm{opt}}\right) \quad (28)$$

5.2 BER Analysis for Pre-Equalization with Bit Loading

In (11), $E'_{\mathrm{b,k}} = d^2(M_k^2-1)/12\log_2 M_k$ and $N'_{0,k} = 1/\alpha_{\mathrm{W/A}}^2\alpha_{\mathrm{A/W}}^2 \times N_0/2$. Following the union bound estimate in (25), the BER for using pre-equalization is estimated as

$$\mathrm{BER}_{\mathrm{pre}} \approx \frac{4}{b_{\mathrm{OFDM}}}\sum_{k=1,3,\ldots}^{N/2-1}\frac{(M_k-1)}{M_k}\times Q\left(\sqrt{\frac{1}{N_0}}\alpha_{\mathrm{W/A}}\alpha_{\mathrm{A/W}}d\right) \quad (29)$$

Next, the optical transmit power can be computed as (16), where $E_{\mathrm{s},k}^{\mathrm{pre}} = d^2(M_k^2-1)/6\times 4/(N|H_k|^2)$ using (11). Hence, the mean optical transmit power is

$$P_{\mathrm{opt}}^{\mathrm{pre}} = \alpha_{\mathrm{W/A}}\sqrt{\frac{1}{\pi NT}}\times\sqrt{\sum_{k=1,3,\ldots}^{N/2-1}\frac{d^2(M_k^2-1)}{6}\frac{4}{N|H_k|^2}} \quad (30)$$

The finalized BER expression in terms of the optical transmit power and the transmission bit rate can be obtained by substituting d in (30) to (29), and substituting $T = b_{\mathrm{OFDM}}/(N+N_{\mathrm{CP}})R$. Thus, the BER expression can be presented as follows.

$$\mathrm{BER}_{\mathrm{pre}} \approx \frac{4}{b_{\mathrm{OFDM}}}\sum_{k=1,3,\ldots}^{N/2-1}\frac{(M_k-1)}{M_k}\times Q\left(\sqrt{\frac{3\pi N b_{\mathrm{OFDM}}}{2N_0(1+N_{\mathrm{CP}}/N)R\sum_{l=1,3,\ldots}^{N/2-1}\frac{(M_l^2-1)}{|H_l|^2}}}\times \alpha_{\mathrm{A/W}}P_{\mathrm{opt}}\right) \quad (31)$$

5.3 BER Analysis for Partial Pre-Equalization with Bit Loading

In (13), $E'_{\mathrm{b,k}} = d^2(M_k^2-1)/12\log_2 M_k$ and $N'_{0,k} = 1/(\alpha_{\mathrm{W/A}}^2\alpha_{\mathrm{A/W}}^2|H_k|^2/|\widehat{H}_k|^2) \times N_0/2$. Following the union bound estimate in (25), the BER for using pre-equalization is estimated as

$$\mathrm{BER}_{\mathrm{partial}} \approx \frac{4}{b_{\mathrm{OFDM}}}\sum_{k=1,3,\ldots}^{N/2-1}\frac{(M_k-1)}{M_k}\times Q\left(\sqrt{\frac{1}{N_0}}\frac{\alpha_{\mathrm{W/A}}\alpha_{\mathrm{A/W}}|H_k|}{|\widehat{H}_k|}d\right) \quad (32)$$

Next, the optical transmit power can be computed as (16), where $E_{\mathrm{s},k}^{\mathrm{pre}} = d^2(M_k^2-1)/6\times 4/(N|\widehat{H}_k|^2)$ using (13). Hence, the mean optical transmit power is

$$P_{\mathrm{opt}}^{\mathrm{partial}} = \alpha_{\mathrm{W/A}}\sqrt{\frac{1}{\pi NT}}\times\sqrt{\sum_{k=1,3,\ldots}^{N/2-1}\frac{d^2(M_k^2-1)}{6}\frac{4}{N|\widehat{H}_k|^2}} \quad (33)$$

The finalized BER expression in terms of the optical transmit power and the transmission bit rate can be obtained by substituting d in (33) to (32), and substituting $T = b_{\mathrm{OFDM}}/(N+N_{\mathrm{CP}})R$. Thus, the BER expression can be presented as follows.

$$\mathrm{BER}_{\mathrm{partial}} \approx \frac{4}{b_{\mathrm{OFDM}}}\sum_{k=1,3,\ldots}^{N/2-1}\frac{(M_k-1)}{M_k}\times Q\left(\sqrt{\frac{3\pi N b_{\mathrm{OFDM}}}{2N_0(1+N_{\mathrm{CP}}/N)R|\widehat{H}_k|^2\sum_{l=1,3,\ldots}^{N/2-1}\frac{(M_l^2-1)}{|\widehat{H}_l|^2}}}\times \alpha_{\mathrm{A/W}}|H_k|P_{\mathrm{opt}}\right) \quad (34)$$

6. NUMERICAL RESULTS

Numerical results are obtained using computer simulation based on the MATLAB software [21]. The simulation parameters are presented in Table 1. In our investigation, the CIRs are varied through the

Table 1: *System parameters for simulation of ACO-OFDM Transmissions*

Parameter	Notation	Value
Bit rate	R	40 Mbps
Actual delay spread	$D_{\text{partial/pre/post}}$	10 ns
Estimate delay spread	$D_{\text{est, partial}}$	2-20 ns
optical transmit power	P_{opt}	10-40 dBm
Number of OFDM subcarriers	N	64
Length of CP	N_{CP}	8
DC gain for CIR	$H(0)$	10^{-6}
PSD of AWGN	N_0	$3.05 \times 10^{-23}\text{A}^2/\text{Hz}$
Number of bits/ OFDM symbol	b_{OFDM}	72
Receiver responsitivity	$\alpha_{\text{A/W}}$	0.53 A/W
Source conversion factor	$\alpha_{\text{W/A}}$	1 W/A
Target BER	BER	10^{-5}

change of the delay spread, which is directly related to the parameter a in (4) for the ceiling bounced model.

In Table 1, the delay spread values follow the typical values in the range of 2-20 ns, as indicated in [1] (see Fig. 13(b)). The number of OFDM subcarriers is set to 64, which is common for wireless local area networks (WLANs), as considered in [5] and mentioned in [6] (see Section III). The length of CP is set equal to 8, which is sufficiently long for the mentioned delay spreads. The DC gain of 10^{-6} follows the typical range indicated in [1] (see Fig. 7(b)) for diffuse OWC channels. The noise variance is selected in the order of $10^{-23}\text{A}^2/\text{Hz}$, as pointed out in [1] (see Fig. 9). The number of bits per OFDM symbol is set to 72 to avoid the use of excessively large QAM constellations, which are not as power efficient for ACO-OFDM [8]. The receiver's responsitivity follows a typical value mentioned in [1] (see Fig. 9) and [5]. The source conversion factor is assumed to be unity for simplicity and without loss of generality; it can be varied by changing the number and/or the type of LEDs used in the transmitter. Finally, the target BER is set to 10^{-5}, and not lower, since uncoded transmissions are assumed.

6.1 BER Performance Comparison without Bit Loading

Fig. 1 and Fig. 2 plot the BER versus the optical transmit power for single-user ACO-OFDM transmissions by comparing the use of partial pre-equalization, pre-equalization, and post-equalization. For the results, it is assumed that $D_{\text{partial/pre/post}} = 10$ ns and that $D_{\text{est, partial}} = D_{\text{partial}}$, i.e., accurate channel knowledge. In each figure, analytical results are plotted as lines while simulation results are shown using markers. It is assumed that 2×2 QAM constellations are used on all subcarriers. At the BER target of 10^{-5} for the data rates of 40 Mbps, both pre- and partial pre-equalization can reduce the required optical transmit power over the use of post-equalization by approximately 4 dB and 3 dB for ACO-OFDM transmission with the ceiling bounced CIR and with the exponential CIR respectively. In addition, both figures verify that partial pre- and pre-equalization have the same power efficiency when the estimated delay is equal to the actual delay. Finally, Fig. 1 and Fig. 2 validate the BER expressions derived in Section 3.4 through a close match between analytical and simulation results.

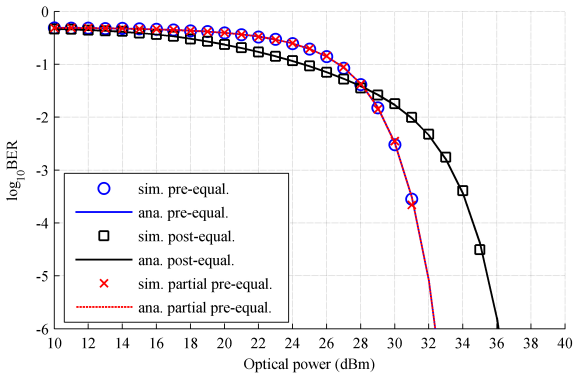

Fig. 1: *BER vs. optical transmit power for ACO-OFDM without bit loading for the ceiling bounced CIR.*

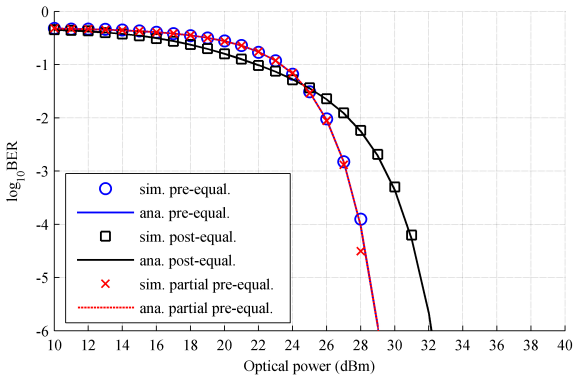

Fig. 2: *BER vs. optical transmit power for ACO-OFDM without bit loading for the exponential CIR.*

6.2 BER Performance Comparison without Bit Loading and with Imperfect Channel Knowledge

For indoor OWC, the optical channels differ in several key ways such as the change of the delay spreads D caused by the position changing between transmitter and receiver as well as propagation characteristics in indoor environments. This section presents the BER performances when the channel knowledge is inaccurate at the transmitter. Fig. 3 plots the BER versus the optical transmit power using partial pre-equalization based on the estimated delay spread of 5, 15, and 20 ns at 40 Mbps compared with pre-equalization and post-equalization operating with accurate channel knowledges.

In Fig. 3, the simulation results are obtained using the ceiling bounced CIR. It is shown that, at the target BER of 10^{-5}, partial pre-equalization requires less optical transmit power than post-equalization even though it is operated based on an imperfect channel estimate, i.e., in case of the worse channel estimate with delay spread of 20 ns. However, the reduction in the optical transmit power depends on the estimated delay spread at the transmitter.

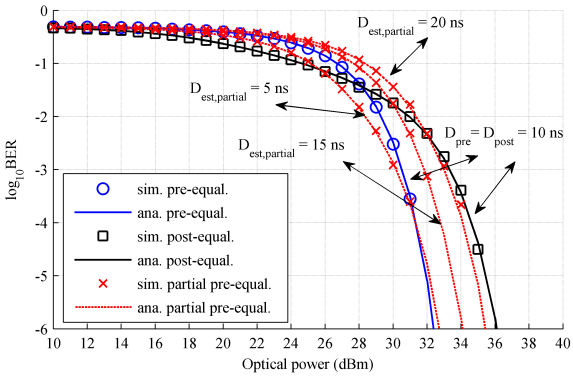

Fig.3: *BER vs. optical transmit power for ACO-OFDM without bit loading and with imperfect channel knowledge for the ceiling bounced CIR.*

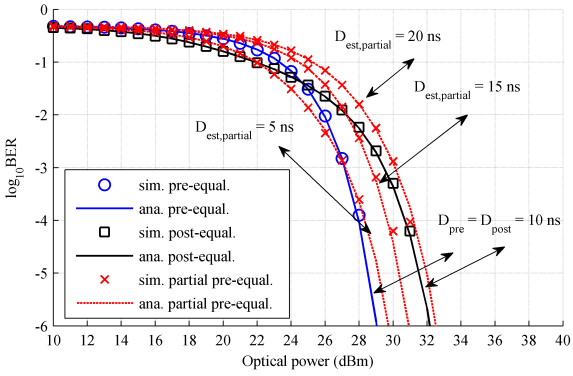

Fig.4: *BER vs. optical transmit power for ACO-OFDM without bit loading and with imperfect channel knowledge for the exponential CIR.*

Fig. 4 plots the same information as in Fig. 3, but with the exponential CIR instead of the ceiling bounced CIR. The results show that there is a reduction in the optical transmit power for partial pre-equalization when compared with post-equalization except for the worst case with the delay spread of 20 ns, where partial pre-equalization requires a slightly higher optical transmit power. However, the difference is insignificant.

6.3 BER Performance Comparison with Bit Loading

Fig. 5 and Fig. 6 plot the BER versus the optical transmit power for single-user ACO-OFDM transmissions with bit loading by comparing the use of partial pre-equalization, pre-equalization, and post-equalization, which is similar to Fig. 1 and Fig. 2.

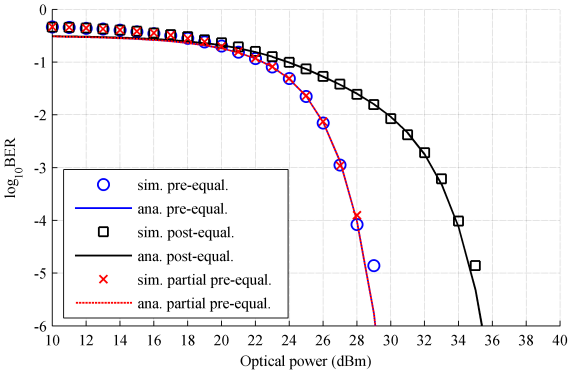

Fig.5: *BER vs. optical transmit power for ACO-OFDM with bit loading for the ceiling bounced CIR.*

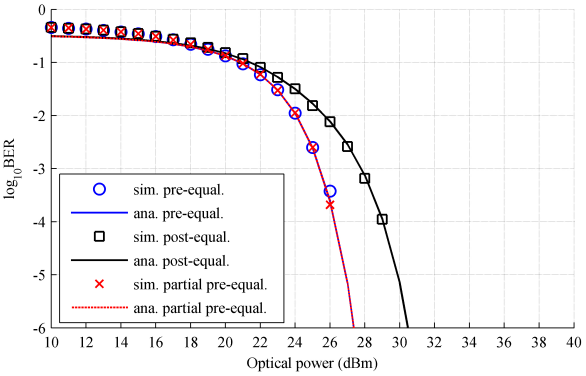

Fig.6: *BER vs. optical transmit power for ACO-OFDM with bit loading for the exponential CIR.*

In each figure, analytical results are plotted as lines while simulation results are shown using markers. At the target BER of 10^{-5} for the data rates of 40 Mbps, partial pre-equalization can reduce the required optical transmit power over the use of post-equalization by approximately 6 dB and 4 dB for ACO-OFDM transmission with the ceiling bounced CIR and with the exponential CIR respectively. Note that the power reductions are similar to Fig. 1 and

Fig. 2. In addition, both figures verify that partial pre- and pre-equalization have the same power efficiency when the estimated delay is equal to the actual delay, i.e., accurate CIR knowledge at the transmitter.

6.4 BER Performance Comparison with Bit Loading and with Imperfect Channel Knowledge

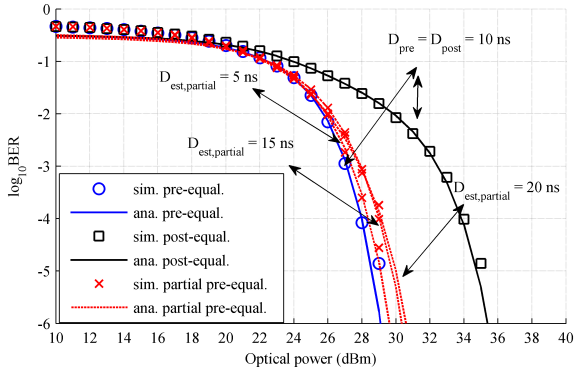

Fig.7: *BER vs. optical transmit power for ACO-OFDM with bit loading and with imperfect channel knowledge for the ceiling bounced CIR.*

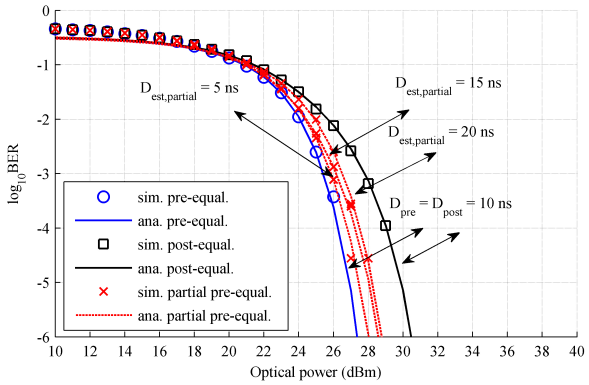

Fig.8: *BER vs. optical transmit power for ACO-OFDM with bit loading and with imperfect channel knowledge for the exponential CIR.*

Fig. 7 plots the BER versus the optical transmit power using partial pre-equalization based on the estimated delay spread of 5, 15, and 20 ns at 40 Mbps compared with pre-equalization and post-equalization, assuming that the latter two schemes are operated with accurate channel knowledges. For post-, pre- ,and partial pre-equalization, the bit loading procedure can be viewed in Section 4.

The simulation results are obtained using the ceiling bounced CIR. It is shown that partial pre-equalization requires a lower optical transmit power than post-equalization. In addition, bit loading helps to reduce the optical transmit power requirement as well. However, the amount of optical power reduction depends on the estimated delay spread at the transmitter.

Fig. 8 plots the same information as in Fig. 7, but with the exponential CIR instead of ceiling bounced CIR. Observe that partial pre-equalization still offers the reduction in the required optical transmit power compared with post-equalization under bit loading. It is interesting to observe that, while an imperfect CIR knowledge may make partial pre-equalization less power efficient than post-equalization (see Fig. 4 for $D_{\text{est, partial}} = 20$ ns), bit loading helps make partial pre-equalization outperform in all cases of estimated delay spread in the considered typical range.

6.5 BER Performance of Partial Pre-Equalization for Broadcast Transmissions to Multiple Users

As mentioned in Section 1, partial pre-equalization not only reduces the required optical transmit power compared to post-equalization, it also supports broadcast transmissions to multiple users with different CIRs while pre-equalization is not applicable. Fig. 9 and Fig. 10 plot the BER versus the actual delay spread for partial pre-equalization with the estimated delay varying from 2 to 20 ns at 40 Mbps and the optical transmit power of 30 dBm for the ceiling bounced CIR and for the exponential CIR, respectively.

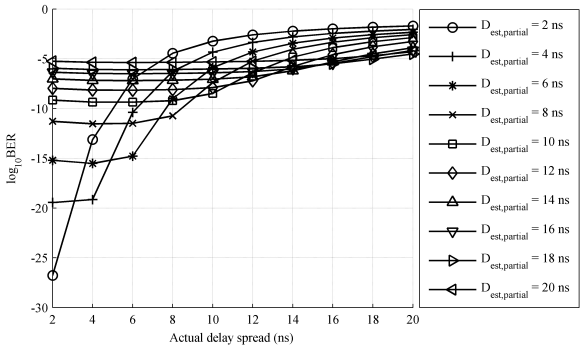

Fig.9: *BER vs. actual delay spread with optical transmit power of 30 dBm at 40 Mbps for the ceiling bounced CIR with $D_{est,partial}$ = 2 to 20 ns.*

For ease of reading, the plots are based only on analytical results. It is interesting to observe that, while using a low estimated dalay spread, e.g., $D_{\text{est, partial}} = 2$ ns, can lead to a better BER performance at low actual delay spreads, it cannot provide a BER below the target of 10^{-5} when the actual delay spreads are high, e.g., 20 ns. Overall, the results indicate that partial pre-equalization should operate based on a conservative worst-case estimate on the delay spread of the CIR, i.e., 20 ns, to guarantee that all users can achieve the target BER of 10^{-5}.

Note that eye safety considerations limit the average optical power which can be transmitted. Accord-

ing to the International Electrotechnical Commission (IEC) (IEC60825-1) standard which provides guidelines on LED and laser emissions [22], the allowable average optical transmit power should be less than 30 dBm.

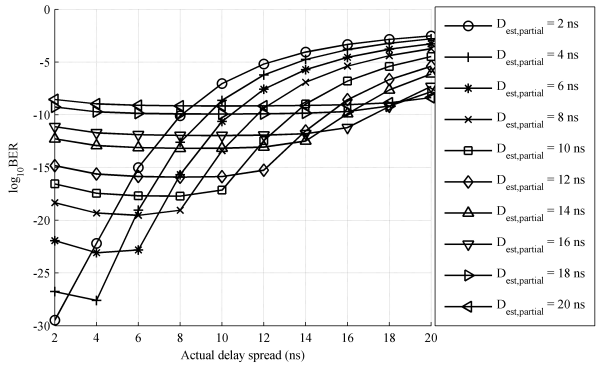

Fig.10: *BER vs. actual delay spread with optical transmit power of 30 dBm at 40 Mbps for the exponential CIR with* $D_{est,partial} = 2$ *to 20 ns.*

7. CONCLUSION

This paper demonstrated that, similar to pre-equalization, partial pre-equalization can offer a significant reduction in the required optical transmit power over post-equalization for ACO-OFDM transmissions over dispersive OWC channels. However, unlike pre-equalization, partial pre-equalization can also be applied in two practial scenarios where pre-equalization is not applicable. The first scenario involves transmissions to a single receiver but with imperfect CIR knowledge at the transmitter. The second scenario involves broadcast transmissions to multiple receivers with possibly different CIRs. In addition, in broadcasting to multiple users, it is best to apply a conservative estimate on the delay spread, i.e., overestimation, in order to guarantee the target BER for all the users. Moreover, it is shown that bit loading can further reduce the required optical transmit power over dispersive OWC channels.

References

[1] Kahn, J.M., Barry, J.R.: "Wireless infrared communications," *Proc. of IEEE*, Feb. 1997, **85**, (2), pp. 265−298.

[2] Elgala, H., Mesleh, R., Haas, H.: "Indoor broadcasting via white LEDs and OFDM" *IEEE Trans. on Cons. Electron.*, Aug. 2009, **55**, (3), pp.1127−1134.

[3] Tanaka, Y., Komine, T., Haruyama, S., Nakagawa, M.: "Indoor visible light data communication system utilizing white LED lights," *IEICE Trans. on Comm.*, Aug. 2003, **E86−B**, (8), pp. 2440−2454.

[4] Afgani, M.Z., Haas, H., Elgala, H., Knipp, D.: "Visible light communication using OFDM," *2nd Inter. Con. on TRIDENTCOM 2*, Mar. 2006, Spain.

[5] Li, X., Vucic, J., Jungnickel, V., Armstrong, J.: "On the capacity of intensity-modulated direct-detection systems and the information rate of ACO-OFDM for indoor optical wireless applications," *IEEE Trans. Comm.*, Mar. 2002, **60**, (3), pp. 799−809.

[6] Armstrong, J.: "OFDM for optical communications," *Jour. of Lightw. Tech.*, Feb. 2009, **27**, (3), pp. 189−204.

[7] Fernando, N., Hong, Y., Viterbo, E.: " Flip-OFDM for optical wireless communications," in *Proc. of 2011 IEEE ITW*, Oct. 2011, Brazil.

[8] Armstrong, J., Schmidt, B.J.C.: "Comparison of asymmetrically clipped optical OFDM and DC-biased optical OFDM in AWGN," *IEEE Comm. Lett.*, May 2008, **12**, (5), pp. 343−345.

[9] Dissanayake, S.D., Armstrong, J.: "Comparison of ACO-OFDM, DCO-OFDM and ADO-OFDM in IM/DD systems," *Jour. of Lightw. Tech.*, Apr. 2013, **31**, (7), pp.1063−1072.

[10] Kanthalue, S., Nanan, P.: "Pre- and post- equalization technique combining for wireless comm.," *Inter. Con. on Info. Netw.*, Jan. 2013, pp. 336−340.

[11] Fazel, K., Kaiser, S.: *Multi-Carrier and Spread Spectrum Systems from OFDM and MC-CDMA to LTE and WiMAX.*, John Wiley & Sons, Ltd, 2008.

[12] Hanzo, L., Munster, M., Chol, B.J., Keller, T.: *OFDM and MC-CDAM for Broadband Multi-User Communications, WLANs and Broadcasting.*, Wiley, 2003.

[13] Saengudomlert, P.: "On the benefits of pre-equalization for ACO-OFDM and flip-OFDM indoor wireless optical transmissions over dispersive channels," *Jour. of Lightw. Tech.*, Jan. 2014, **32**, (1), pp.70−80.

[14] Wilson, S.K., Armstrong, J.: "Transmitter and receiver methods for improving asymmetrically-clipped optical OFDM," *IEEE Trans. on Wireless Comm.*, Sep. 2009, **8**, (9), pp.4561−4567.

[15] Panta, J., Saengudomlert, P., Sripimanwat, K.: "Performance analysis of partial pre-equalization for ACO-OFDM indoor optical wireless transmissions," *9th Inter. Sym. on Comm. Netw. and Digi. Sign. Proc. (CSNDSP)*, July 2014, pp.1029−1033.

[16] Mesleh, R., Elgala, H., Haas, H.: "On the performance of different OFDM based optical wireless communication systems," *IEEE/OSA Jour. of Optic. Comm. and Netw.*, Aug. 2011, **3**, (8), pp.620−628.

[17] Carruthers, J., Kahn, J.: "Modeling of nondi-

rected wireless infrared channels," *IEEE Trans. on Comm.*, 1997, **45**, (10), pp.1260−1268.

[18] Armstrong, J., Lowery, A.J.: "Power efficient optical OFDM," *Electron. Lett.*, Mar. 2006, **42**, (6), pp. 370−372.

[19] Proakis, J.G., Salehi, M.: *Digital Communications.* McGraw-Hill, 2008.

[20] Ko, H., Lee, K., Oh, S., Kim, C.: "Fast optimal discrete bit-loading algorithms for OFDM-based systems.," *Proc. of 18th Inter. Con. on Com. Comm. and Netw. (ICCCN)*, Aug. 2009, pp. 1−6.

[21] MATLAB, www.mathworks.com/products/matlab/

[22] Hranilovic, S.: *Wireless Optical Communication Systems.* Springer, Boston, 2005.

Keattisak Sripimanwat graduated in B.s (Physics) from Chiangmai University, and M.Eng (Electrical) from King Mongkut's Institute of Technology Ladkrabang (KMITL) in 1989 and 1994 respectively. He received an employee of the year award from a telephone public company in Bangkok during his engineering carrier from 1994 to 1996. He continued for D.Eng (Telecommunications) at Asian Institute of Technology (AIT) and graduated in 2000. He was a one-year visiting scholar at Vienna University of Technology (TU-Wien), Austria, and another half-year researcher at TRLabs (Telecommunications Research Laboratories) Edmonton AB, Canada. He was a researcher at Nectec from 2001- June 2015. His interests are on quantum cryptography and visible light communications where both are found later being consortiums in Thailand (Q-Thai.Org & LED-SmartCoN.Org) and chairing by him. He is a volunteer, an IEEE senior member, and was a chair of IEEE communications society (Thailand chapters) including a general secretary of ECTI association. He has been serving as an editor of Thai telecommunications knowledge management (TTKM), and published various books ("Turbo codes applications" by Springer-2005, and many of them serving free of charge at www.thaitelecomkm.org/ks), and a number of papers including pending patents.

Jariya Panta received the AIT fellowship to obtain her masters of engineering degree (M.Eng.) in Telecommunications from the school of engineering and technology, Asian Institute of Technology (AIT), Pathumthani, Thailand, in 2014. Ms. Jariya received her bachelor of engineering (B.Eng.) from the Department of Electrical and Electronic Engineering, Faculty of Engineering, Ubon Ratchathani University (UBU), Ubon Ratchathani , Thailand, in 2011. During her undergraduate studies she received internship training on optical wireless communications (OWC) at National Electronics and Computer Technology Center (NECTEC),Pathumthani, Thailand. She is currently a Lecturer at Faculty of Industrial Technology , Ubon Ratchathani Rajabhat University (UBRU), Thailand. Her research areas include wireless communications, optical communications, and mobile communications.

Poompat Saengudomlert received the scholarship from His Majesty the King of Thailand to obtain the B.S.E. degree in Electrical Engineering from Princeton University, USA, in 1996. He then obtained the M.S. and Ph.D. degrees, both in Electrical Engineering and Computer Science, from Massachusetts Institute of Technology (MIT), USA, in 1998 and 2002 respectively. From January 2005 to April 2013, he served as an Assistant and then Associate Professor in Telecommunications at Asian Institute of Technology (AIT), Thailand. Since May 2013, he has been serving as an Associate Professor in Telecommunication Engineering at BU-CROCCS (Bangkok University's Center of Research on Optoelectronics, Communications, and Control Systems), Thailand. His research interest includes communication theory, optical communications, and network optimization.